BNL-105291-2014-CP

Investigation of Heat Pipe Cooling Of LI-ION Batteries

Andrey Belyaev, Dmitriy Fedorchenko, Manap Khazhmuradov, Alexey Lukhanin,
Oleksandr Lukhanin, Yegor Rudychev
Kharkov institute of physics and technology, Ukraine
Bahram Khalighi, Taeyoung Han, Erik Yen
Vehicle Systems Research Laboratory GM R&D Center
General Motors Global R & D
Upendra S. Rohatgi
Brookhaven National Laboratory, USA

Presented at the ASME 2014
International Mechanical Engineering Congress & Exposition (IMECE 2014)
November 14 – 20, 2014

May 2014

Nonproliferation and National Security Department

Brookhaven National Laboratory
P.O. Box 5000
Upton, New York 11973
www.bnl.gov

DISCLAIMER

INVESTIGATION OF HEAT PIPE COOLING OF LI-ION BATTERIES

Andrey Belyaev, Dmitriy Fedorchenko, Manap Khazhmuradov, Alexey Lukhanin, Oleksandr Lukhanin, Yegor Rudychev
Kharkov institute of physics and technology, Ukraine
Bahram Khalighi, Taeyoung Han, Erik Yen
Vehicle Systems Research Laboratory GM R&D Center
General Motors Global R & D
Upendra S. Rohatgi
Brookhaven National Laboratory, USA

ABSTRACT

Li-Ion batteries are currently used in hybrid and electric vehicles. Battery life and performance requires temperature control in narrow range. One of the method considered is use of specially designed heat pipe. The study includes a heat pipe between two battery simulators. The heat pipe was cooled by air flow of 3 l/s and with temperature range of from 9°C to 40°C.

We have compared the measured surface temperature distributions to those which were received from computer simulation in order to obtain effective thermal conductivity of the heat pipe and its thermal performance. This effective thermal conductivity increases, as the inlet air temperature increases and reaches the value of 2500 W/(m×K).

INTRODUCTION

Nowadays, Li-Ion batteries are widely used as power sources for various devices. But theese batteris have tight restrictions on the working temperature, especially for charging mode. The most efficient charging regime of Li-Ion batteries ocuurs in rather narrow temperature ragnge of 30 – 35 °C and volume temperature gradient of several degrees of Celsium [1]. For the temperatures above 40°C the battery life decreases, while below 10°C the battery performance degrades and working efficiency substantially decreases.

The heat generation in the Li-ion battery cell depends on the charge/discharge current, which increases with battery use time. We chose the value of the maximum heat generation of 15 watts per each Li-ion battery cell, based on the available calculations and the experimental results [2,3].

Tthe efficiency of Li-Ion battery cooling process using the heat pipe has been investigated. Cooling efficiency for such system depends on the thermal conditivity of the heat pipe, inlet air temperature and flow rate. The operational performance of cooling system for the temperature range from 9 to 40°C and working regime of heat pipe for these temperatures have been studied.

EXPERIMENTAL SETUP

The experimental setup for studies of cooling system performance includes measurement chamber, power source for battery imitators, air station, airflow rate and temperature measurement system and surface temperature measurement system. The entire setup is schematically shown on the Fig. 1.

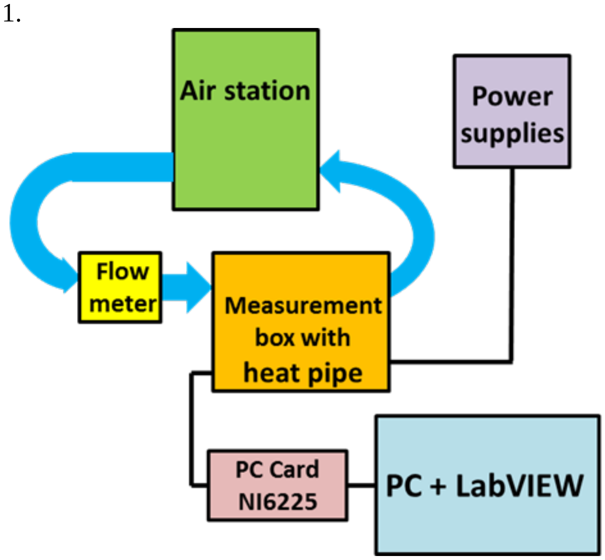

Fig. 1. *Block diagram of the experimental setup for the measurement chamber with heat pipe.*

Instead of the Li-Ion batteries we have used two battery power cells imitators with thermal properties equivalent to the real ones, which were developed earlier [4]. The overall dimension of the cells were 200×150×12 mm.

To study the cooling process measurement chamber for two power cells and a heat pipe was constructed. The gap between the cells was 3 mm. The heat power of each power cell imitator was 7.5 W.

The flat heat pipe size is 220×200×3 mm. It was placed between the power cells. To improve the thermal contact between power cell and heat pipe we used the heat-conducting paste with thermal conductivity of 1 W/ (m×K). The "hot end" of the heat pipe with the radiator is placed in the airflow channel.

The air station provides the inlet airflow rates up to 80 m^3/h, with the temperatures ranging from -20 °C to +50°C. The measuring system was based on the NI6225 PC-card and LabView software. It was monitoring the surface temperature of the imitators. The surface temperature distribution was (mapped) obtained using temperature sensors TMP36. Each simulator surface holds 20 such sensors.

The heat pipe, imitators and air channel were heat-insulated from the environment. The air flow, with stabilized temperature, passes through the radiator ribs or fins in the upper part of the heat pipe and removes heat. For the airflow rate of 3 l/s the pressure drop in the air channel DP (air) was 28 Pa for all inlet air temperatures. The design of the measurement chamber is shown on the figure 2.

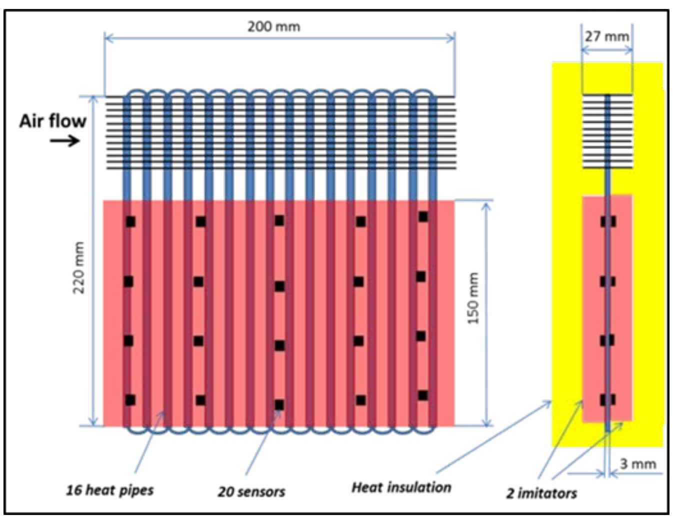

Fig. 2. *Measurement chamber with heat pipe.*

The heat pipe is based on thermo-siphon principle. It consists of 16 thin heat pipes, which are joined in one condensation/evaporation module. Each pipe is made of stainless steel and has diameter of 4 mm with 0.3 mm wall thickness. As the gap between the simulators is 3mm we have to pre-press these cylindrical pipes so they fit inside the channel, and due to the elliptical pipe deformation width becomes 5 mm.

The pipe has inner layer made from stainless steel mesh with mesh size of 0.12mm×0.14mm. This layer provides separation of the vapor and liquid flows and ensures perfect wetting of the side wall. Figure 3 shows the actual heat pipe design.

Fig. 3. *The actual heat pipe photo.*

EXPERIMENTAL RESULTS

Using our experimental setup we have studied the cooling process for inlet air temperature range from 9°C to 40°C. In all cases the airflow rate was 3 l/s. The heat pipe used butane as working liquid. The main subject of our interest was surface temperature distribution for the power cell imitators. This distribution provides information about average battery temperature regimes and temperature gradients. The measured surface temperature distributions for inlet air temperatures 20°C and 30°C are shown on the Figure 4. Table 1 contains minimal, maximal and average surface temperatures for the different air velocities.

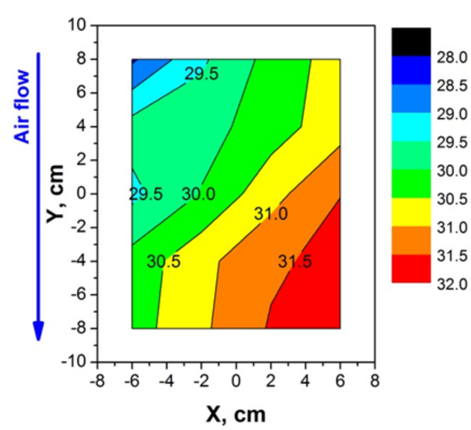

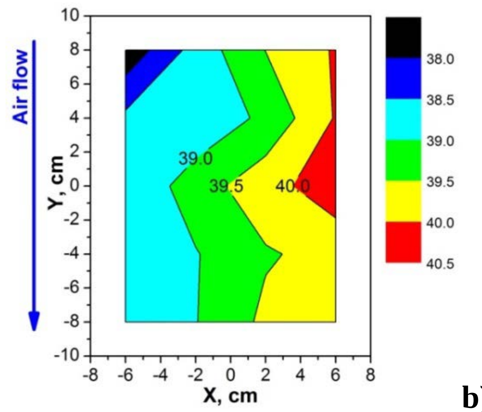

b),

Fig. 4. *The temperature distribution of one simulator surface, at 3 l/sec air flow rate. Inlet air temperature: a) – 20 °C, b) – 30.0 °C.*

Table 1. The measurement minimum, maximum and average temperatures for two surfaces of the imitators.

T(air), °C	T(min), °C		T(max), °C		T(avg), °C	
	1	***2***	***1***	***2***	***1***	***2***
9.0	19.2	19.2	21.1	21.1	20.3	20.3
20.0	28.7	28.4	31.7	31.7	30.5	30.5
30.2	37.8	37.6	40.1	40.3	39.2	39.2
38.6	46.9	46.9	48.2	48.2	47.6	47.6

There are a number of ways to quantitatively estimate cooling efficiency. In our paper we adopt Q/ITD as such parameter. This parameter is defined as;

Where Q is heat power, T_{avg} – average surface temperature, T_{inlet} – inlet air temperature. The denominator in (1) is often called ITD –Inlet Temperature Difference. Using the experimental data from table 1 we obtain cooling efficiency of the heat pipe (see Fig. 5).

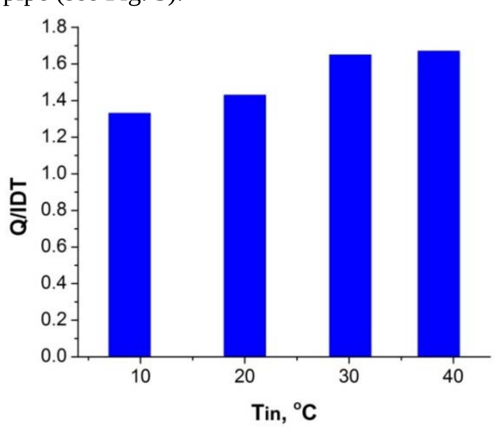

Fig. 5. *The cooling efficiency for heat pipe.*

The slight dependency of the cooling efficiency on the inlet air temperature is connected with the changes of vapor pressure and velocity inside the heat pipe.

NUMERICAL SIMULATION AND ANALYSIS

Numerical simulation of the cooling system included two stages. During the first stage we have simulated evaporation and convection in the single tube out of the 16 tubes forming the heat pipe. Our aim was to analyze vapor flow inside the heat pipe, namely, pressure and velocity distribution. On the next stage we considered the entire cooling system, but we neglected the details of heat transfer inside the heat pipe. This stage helps us to estimate the effective thermal conductivity by comparing results with the experimental results. All simulations were performed using SolidWorks 2011 software with SolidWorks Flow Simulation module.

The model for single tube was rectangular parallelepiped with full length of 170 mm and 2mm×4mm cross section. It consisted of evaporation area (l_e=150 mm) and adiabatic area (l_a=20 mm). Our software does not directly support simulation of evaporation process. Thus we manually set the boundary conditions for the evaporation area as inlet mass flow. The corresponding mass flow rate is defined by the heat power applied to the pipe and by evaporation heat of the working liquid. In our case we have heat power of 0.93 W, and for butane we obtain the required mass flow rate of $0.24\cdot10^{-5}$ kg/s. As we have to consider the evaporation process at the working temperature 20°C, we have specified the butane pressure of 200 kPa.

During the simulation we have used meshes containing 48384, 176640 and 573120 cells to decrease the uncertainties due to discretization. The control parameter was average vapor velocity on the outlet. According to the procedure described in [5] the grid convergence index (GCI) was 3.65%.

Figure 6 contains pressure and vapor velocity distributions in the heat pipe. One can see that flow velocity is rather low and so the corresponding pressure drop due to hydrodynamic drag is low and does not have a substantial effect on the heat transfer.

Considering the working characteristics of the heat pipe using thermo-siphon principle one also must estimate the entrainment limit [5]. This limit is caused by the condenser flooding. The corresponding relation for heat transfer limit is given by

$$Q_{\max} = \mathrm{Ku}\,(\rho_v)^{0.5}\left[g\,(\rho_l - \rho_v)\sigma_l\right]^{0.25}, \quad (2)$$

Where ρ_l, ρ_v are vapor and liquid densities correspondingly, σ_l is surface tension, g is free fall acceleration, Ku is Kutateladze number. Kutateladze number we calculated using the following relation from [5]

$$\mathrm{Ku} = 0.16\left\{1 - \exp\left[-\left(d_e / l_e\right)\left(\rho_l / \rho_v\right)^{0.13}\right]\right\}, \quad (3)$$

Where d_e, l_e are vapor channel diameter and length. For current heat pipe, formula gives the heat transfer limit of 1.189 W while the required heat power is 0.93 W.

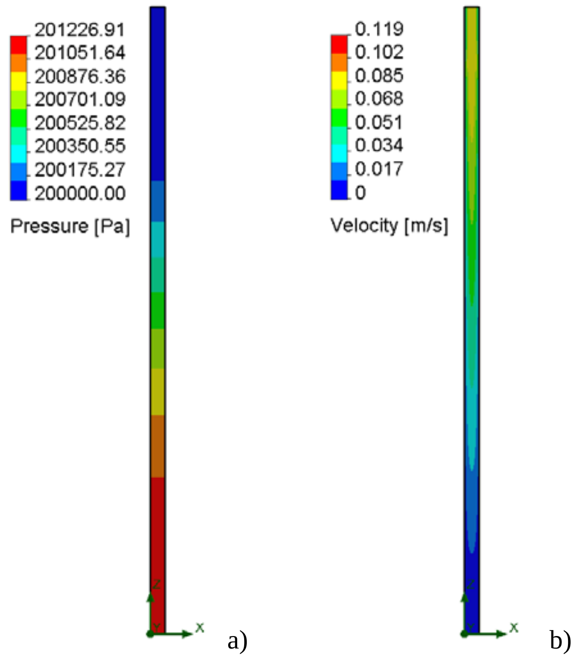

Fig. 6. *Pressure distribution (a) and velocity of butane vapors (b) in the heat pipe at 20 °C*

During the second stage we have developed the 3D model of the cooling system (Fig. 7).

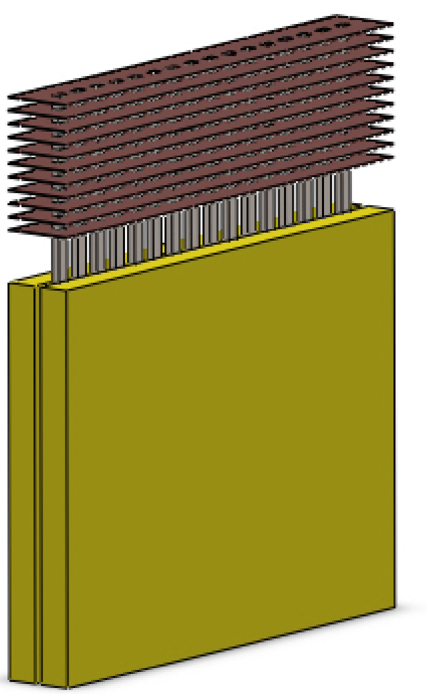

Fig. 7. *CAD model for the cooling heat pipe*

It consisted of two heater plates with thermal properties similar to those of real imitators, 16 rectangular pipes with fixed thermal conductivity and radiator. During calculations we varied thermal conductivity of the heat pipes in order to fit the calculated surface temperature distribution to the experimental. This fitting process was repeated for inlet temperatures. The thermal conductivities results are shown in the table 2 and figure 8.

Table 2. Surface temperatures and heat pipe thermal conductivity (numerical simulation).

T(air), °C	**K,** W/(mK)	**T(min),**°C	**T(max),**°C	**T(avg),**°C
9.0	1100	17.1	21.8	20.3
20.1	1450	27.6	31.9	30.4
30.2	2400	37.0	40.5	39.2
38.6	2600	45.4	48.8	47.6

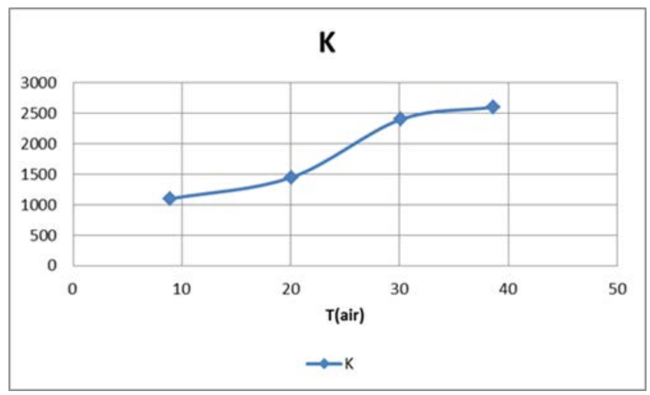

Fig. 8. *Thermal conductivity heat pipe.*

Another point of our interest was air cooling efficiency. To estimate this parameter we have calculated the radiator temperatures (Table 3). Using these results we have estimated the cooling efficiencies and thermal conduction along the cooling system for the following components: imitator-airflow, radiator-airflow, and imitator-radiator (thermal conduction). For cooling efficiency we used Q/ITD parameter defined according to (1), and thermal conduction was defined as

$$q = \frac{Q}{\Delta T}, (4)$$

Where ΔT is temperature drop between imitator and radiator. The results are shown on the figure 9.

Table 3. Radiator temperatures (numerical simulation).

T(air), °C	**T(min),**°C	**T(max),**°C	**T(avg),**°C
9.0	13.4	17.1	15.4
20.1	24.6	28.0	26.6
30.2	34.8	37.8	36.6
38.6	43.4	46.3	45.1

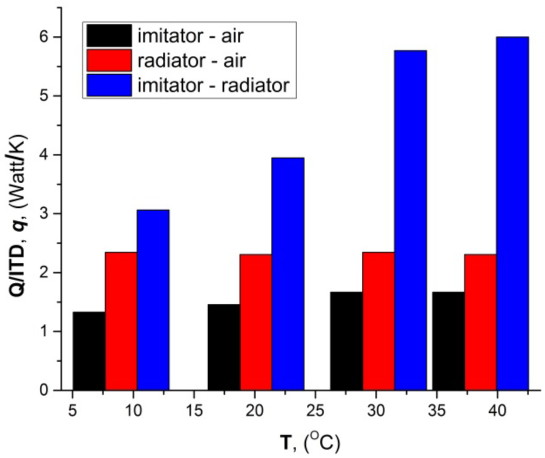

Fig.9. *Dependence of cooling efficiency and thermal conduction coming from inlet air temperature for some chosen heat pipe areas.*

Results of the calculations (Fig. 9) show that the cooling efficiency for the radiator, cooled by inlet air is constant, while thermal conduction of heat pipe increases with the inlet air temperature increase.

CONCLUSIONS AND DISCUSSIONS

We have shown that flat multi-sectional heat pipe provides efficient cooling of the Li-Ion battery. The achieved values of Q/IDT are 1.4 – 1.7 for inlet air temperatures from 9 °C to 40°C, battery working temperature within 20 °C – 47°C range and temperature gradient is about 3°C. The effective thermal conductivity is 1100-2600 W/(m K).

According to the simulation results the highest thermal resistance transition appears at the radiator ribs area cooled by airflow. The further improvement of the cooling efficiency requires the more efficient radiators for heat pipe.

ACKNOWLEDGMENTS

This research investigation was done under Department of Energy program of Global Initiative for Proliferation Prevention grant (BNL-T2-371-UA).

REFERENCES

1. Ahmad Pesaran, Matt Keyser, Gi-Heon Kim, Shriram Santhanagopalan, and Kandler Smith. ***Tools for Designing Thermal Management of Batteries in Electric Drive Vehicles.*** Presented at the Large Lithium Ion Battery Technology & Application Symposia Advanced Automotive Battery Conference; Pasadena, CA. February 4–8, 2013. NREL Report No. PR-5400-57747.
2. Taeyoung Han, Gi-Heon Kim, and Lewis Collins. ***Fast-Charging Battery Development: Multiphysics Simulation Tools Power the Modeling of Thermal Management in Advanced Lithium-Ion Battery Systems for Electric Vehicles.*** ANSYS Advantage. Vol. 6(3), 2012; pp. 10-14; NREL Report No. JA-5400-55941.
3. Ui Seong Kim, Jaeshin Yi, Chee Burm Shin, Taeyoung Han, Seongyong Park, ***Modelling the thermal behaviour of a lithium-ion battery during charge.*** Journal of Power Sources 196 (2011) 5115–5121.
4. Andrey Belyaev, Alexandr Lukhanin, Alexey Lukhanin, Dmitriy Fedorchenko, Manap Khazhmuradov, Igor Rudychev, Upendra S. Rohatgi. ***Thermal Characteristics of Air Flow Cooling in the Lithium Ion Batteries Experimental Chamber.*** Proc. ASME 2012 Heat Transfer Summer Conference, Volume 1: Heat Transfer in Energy Systems; Rio Grande, Puerto Rico, USA, July 8–12, 2012, pp.129-133.
5. ***Procedure for Estimation and Reporting of Uncertainty Due to Discretization in CFD Applications,*** J. Fluids Eng. 130, 078001 (2008); doi: 10.1115/1.2960953.
6. D.A. Reay, P.A. Kew, ***Heat Pipes*** *(Fifth Edition)*, Butterworth-Heinemann, 2006.